RSC Advances

ROYAL SOCIETY
OF CHEMISTRY

www.rsc.org/advances

RSC Advances

ARTICLE

Hydrogen Bonds Breaking of TPU upon Heating: Understanding from the Viewpoint of Molecular Movements and Enthalpy

Qiang Yuan,[a] Tao Zhou,[a],* Lin Li,[b] Jihai Zhang,[a] Xifei Liu,[a] Xiaolin Ke,[a] and Aiming Zhang[a]

Hydrogen bonds breaking of TPU based on 4,4,-methylenediphenyl diisocyanate (MDI)/1,4-butanediol (BDO) upon heating was studied and elucidated from molecular movements and enthalpy. Two temperature regions of hydrogen bonds breaking, including Region I (80−133 °C) and region II (133−169 °C), were determined via the combination of PCMW2D correlation FTIR and DSC. The method of calculating the enthalpy of the hydrogen bonds breaking was established via Van't Hoff plots. We also proposed the method of calculating the relative content of different hydrogen bonds. In region I, ΔH_h =58.8±0.5 kJ/mol for N–H and C=O, and ΔH_h=37.2±0.4 kJ/mol for N–H and C−O−C groups. The content of hydrogen bonds generated by N–H and C=O is 88.4%, and that of N–H and C−O−C is 11.6%. In region II, ΔH_h=65.0±1.1 kJ/mol for N–H and C=O, and ΔH_h=73.0±3.9 kJ/mol for N–H and C−O−C groups. The contents of these two hydrogen bonds are 71.2 % and 28.8%, respectively. The surprised high value of ΔH_h=73.0±3.9 kJ/mol for N–H and C−O−C in region II is actually due to the stabilization of the repulsion energy on hydrogen bonds in the interface. The 2D correlation analysis was used to investigate the sequential order of groups' movement involved in hydrogen bonds breaking. In Region I, the breaking of a small amount of hydrogen bonds between N–H and C−O−C in the interface firstly occurs, and then the breaking of the irregular hydrogen bonds between N–H and C=O in TPU hard blocks is dominated, resulting in the melting of the imperfect crystalline in hard blocks. In Region II, it is firstly the breaking of regular hydrogen bonds between N–H and C=O in the perfect crystalline in hard blocks, and then is followed by the hydrogen bonds breaking of N–H and C−O−C enhanced by the repulsion energy in the interface, leading to the order-disorder transition (ODT) of TPU.

1. Introduction

The thermoplastic polyurethane (TPU) is a typical linear block copolymer which is composed of the alternating soft blocks and hard blocks. Hard blocks and soft blocks are thermodynamically incompatible, and therefore, a micro-phase separation structure is formed.[1, 2] For polyether TPUs, poly(ethylene glycol) (PEG), polyoxypropylene (PPO), or polytetrahydrofuran (PTMEG) are usually used as soft blocks,[1-5] and hard blocks often synthesized from 4,4,-methylenediphenyl diisocyanate (MDI), 2,6-toluene diisocyanate(TDI) and a chain extender, such as 1,4-butanediol (BDO) or butane diamine (BDA).[1-8] TPU has a wide range of applications in various fields, such as foams, coating, life-saving biomedical devices, textile fibers, adhesives, and so on.[1, 2]

A lot of researches have been done in both academia and industry for the past few decades,[1, 2, 9, 10] which focused on the hydrogen bonding, the phase morphology, and thermal transitions of polyether TPUs. Due to the outstanding performance, TPUs which hard blocks are from the reaction product of BDO and MDI, and soft blocks are based on polyether polyols were most frequently studied.[1, 2, 11] The hydrogen bonds are an important part of polyether TPUs based on BDO and MDI. Amine groups (N–H in hard blocks) are proton donors, and carbonyl groups (C=O in hard blocks) and ether groups (C–O in soft blocks) are proton acceptors.[1, 2, 12-14] Thus, two types of hydrogen bonds can be generated. However,
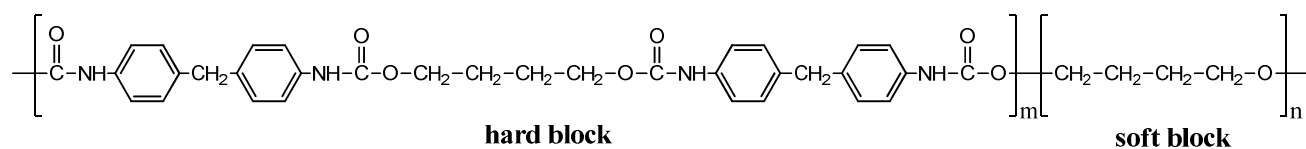
Scheme 1. Chemical structure of polyether TPU used in this study.

because of the phase separation, the formation of hydrogen bonds is mainly between N–H groups and C=O groups in hard blocks. Hydrogen bonds in hard block even can induce an obvious crystallization of hard blocks,[1, 2, 15, 16] which significantly enhances properties of TPUs. The content of hydrogen bonds between N–H groups and C–O–C groups is very small, only existing in the phase interface between the hard and soft blocks. Hydrogen bonds play an important role on the stabilization of TPUs hard blocks, which direct affects the performance of TPUs. The breaking of hard blocks is taken place when the temperature is increased above the order-disorder transition (ODT) temperature.[16-19] The breaking of hydrogen bonds is a main reason of hard blocks dissociation, and another reason is that the interaction parameter between the hard and soft blocks becomes 0 at a high temperature, resulting in a miscibility of two phases. In general, the stronger hydrogen bonds give a higher temperature of ODT temperature. However, the process of hydrogen bonds breaking upon heating has been unclear so far. A depth understanding of hydrogen bonds breaking in TPUs will have a great scientific and practical value.

In the past few decades, many groups tried to figure out the behavior of hydrogen bonds in TPUs. For example, McKiernan investigated the influence of hydrogen bonds on the crystallization behavior of TPUs via designing a series of semicrystalline structure.[20] Emel used the quantum mechanics combined with vibrational spectroscopy to calculate the hydrogen bonding energy of model compounds of TPUs.[21] Fourier transform infrared spectroscopy (FTIR) was used to study hydrogen bonds due to the unique advantage of FTIR.[13, 14, 22] For hard blocks of TPUs, it is commonly known that the N–H stretching vibration in amine groups is composed of two contributions, including "free" (non-hydrogen bonded) and hydrogen bonded N–H groups.[13, 14, 22] Also, the C=O stretching vibration is divided into "free" (non-hydrogen bonded) and hydrogen bonded groups.[13, 14, 22-25] In the earlier study, only limited information on the behavior of hydrogen bonds was gained through the changes of the spectral intensity and the bandwidth of N–H and C=O groups from FTIR. A similar study was also performed to investigate the hydrogen bonding with different molecular structures of hard blocks.[26-28] However, the explanation of the hydrogen bonds breaking from the viewpoint of the enthalpy and molecular movements has not been reported so far.

Generalized two-dimensional (2D) correlation infrared spectroscopy proposed by Noda in 1993 gradually became an important spectroscopy method in the past two decades.[29, 30] One of the benefits for 2D correlation spectroscopy is the

significant enhancement of the spectral resolution. In addition, the 2D correlation infrared spectra can easily provide the sequential order of spectral variables according to Noda's rules.[29, 30] Thus, the 2D correlation infrared spectroscopy is certainly one of the best ways to study polymer transition mechanism. Based on the theory of moving-window two-dimensional correlation spectroscopy (MW2D) reported by Thomas and Richardson,[31] Morita proposed perturbation-correlation moving-window two-dimensional correlation spectroscopy (PCMW2D) in 2006,[32] which can be directly applied to see the spectral correlation variation along both perturbation variables (e.g., temperature) and spectral variables (e.g., wavenumber) axis. The 2D correlation infrared spectroscopy has a natural advantage on the study of the polymer transitions with the hydrogen bonding.[33-39] In the past few years, the combination of PCMW2D and generalized 2D correlation analysis was found to be the best implementation way for the study of the polymer transitions.[34, 35, 38-44] A common practice is that the transition point and the transition region of polymers were first determined by PCMW2D, and then the generalized 2D analysis was carried out to study the sequential orders of the groups' movement at a specific transition.[38-44]

In this study, two temperature regions of hydrogen bonds breaking of TPU upon heating are determined via the combination of PCMW2D and differential scanning calorimetry (DSC). The method of calculating the enthalpy of hydrogen bonds breaking from the temperature-dependent FTIR is also successfully established via Van't Hoff plots. The relationship of the breaking enthalpies of different hydrogen bonds type is proposed, and therefore, the relative content of hydrogen bonds generated by N–H and C=O groups can be estimated quantitatively. The powerful 2D correlation analysis is used to investigate the sequential order of groups' movement involved in hydrogen bonds breaking. In these two regions, the process of hydrogen bonds breaking gained from the enthalpy is the same as the inferred from the 2D correlation analysis.

2. Experimental

2.1. Materials

The commercial polyether TPU (WHT8185) which was bought from Yan Tai Wan Hua Co, Ltd of China was used in the present study. The hard blocks of this polyether TPU were based on 4,4'-diphenylmethane diisocyanate (MDI) extended by 1,4-butanediol (BDO), and the soft blocks were polytetrahydrofuran (PTMEG) with molecule weight of 1000

g/mol. The chemical structure of TPU is provided in **Scheme 1**. The sample was dried at 80 °C for 5 h with a vacuum degree of -0.08 MPa. Tetrahydrofuran (THF) was brought from Cheng Du Ke Long Co. of China, and the purity was 99.8 wt%.

2.2. Differential scanning calorimetry (DSC)

DSC measurement was performed using NETZSCH 204 F1. The sample was first heated from 30 °C to 220 °C at 40 °C/min, and held at 220 °C for 3 min to eliminate the thermal history. Then the sample was cooled from 220 °C to 50 °C at 10 °C/min, kept at 50 °C for 3 min, and finally heated again from 50 °C to 220 °C at 10 °C/min. The measurement was performed under a nitrogen atmosphere (50 mL/min).

Table 1. Band assignments for FTIR spectra of TPU.

| Wavenumber (cm^{-1})	Assignments	
	Hard blocks	**Soft blocks**
3430	v(N−H, free), N−H stretching of "free" N−H groups	--
3332	v(N−H, bonded), N−H stretching of hydrogen-bonded N−H groups	--
1740	v(C=O, free), C=O stretching of "free" C=O groups	--
1700	v(C=O, bonded), C=O stretching of hydrogen-bonded C=O groups	--
1114	--	v_{as}(C–O–C), asymmetrical stretching

2.3. *In situ* FTIR spectroscopy

TPU of 0.5 g was first dissolved in 10 mL THF (50 g/L), and then coated on the one side of KBr disk (Φ13 mm). The KBr disk with TPU film sample was dried at 70 °C for 240 min with a vacuum degree of -0.08 MPa in a vacuum oven. The TPU film thickness was about 12 μm. To prevent the flow of the sample at a high temperature, the TPU film was sandwiched with another piece of KBr disk. After that, the sandwiched film was placed into a homemade in situ pool (programmable heating and cooling device). The sample was first heated from 30 °C to 220 °C at the speed of 5 °C/min, and kept at 220 °C for 3 min to eliminate the thermal history. Then, the sample was cooled from 220 °C to 50 °C at 5 °C /min, and held at 50 °C for 3 min. Finally, the sample was reheated from 50 °C to 205 °C at 5 °C/min. The temperature-dependent FTIR spectra in the region 4000-400 cm^{-1} were collected for the final reheating process using Nicolet iS10 equipped with a deuterated triglycine sulfate detector. A total of 97 FTIR spectra were gathered. The resolution of the spectra was 4 cm^{-1}, and the scans of each FTIR spectrum was 20. To prevent oxidative degradation, the sample was protected by a dried and high-purity nitrogen gas with 300 mL/min.

2.4. 2D correlation analysis

PCMW2D and generalized 2D correlation FTIR spectra were processed, calculated, and plotted by 2DCS software, developed by one of the authors. The window size of PCMW2D was chosen as 15 (*2m+1*) to produce high-quality spectra. The linear baseline corrections were applied in the region of 3490−2520 cm^{-1}, 1860−1650 cm^{-1}, and 1650−880 cm^{-1} before analysis. The 5% correlation intensity of spectra was regarded as noise and was cut off. In 2D correlation FTIR spectra, the pink areas represent positive correlation intensity, and the blue areas represent the negative correlation intensity. The theory and algorithm of PCMW2D and generalized 2D correlation spectroscopy can refer to the literature.[29, 30, 32]
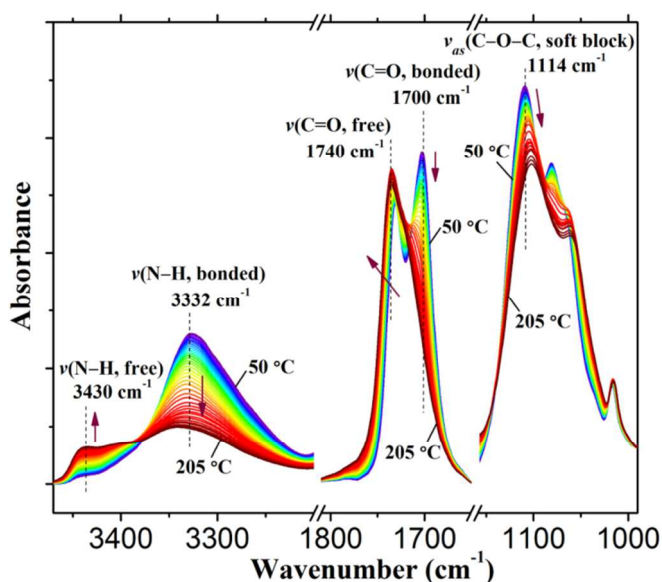
Figure 1. Temperature-dependent FTIR spectra of TPU upon heating from 50°C to 205 °C in the region 3470–3200 cm^{-1} (N–H stretching), 1810–1650 cm^{-1} (C=O stretching), and 1160–990cm^{-1} (C–O–C stretching).
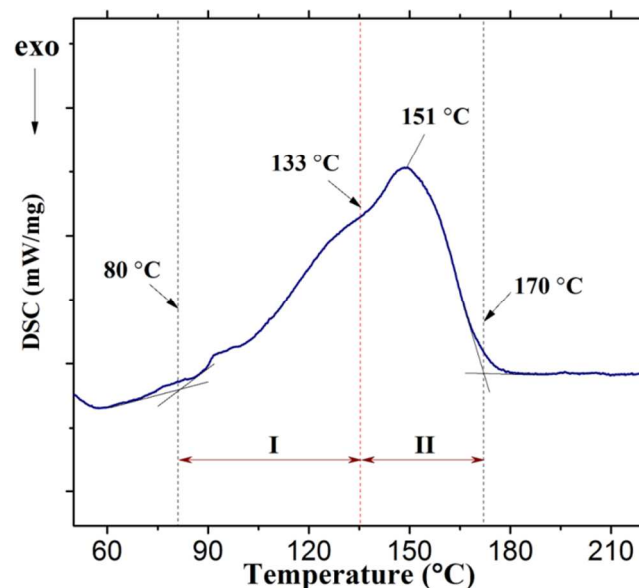
Figure 2. DSC curve of TPU from 50 °C to 220 °C upon heating at 10 °C/min.
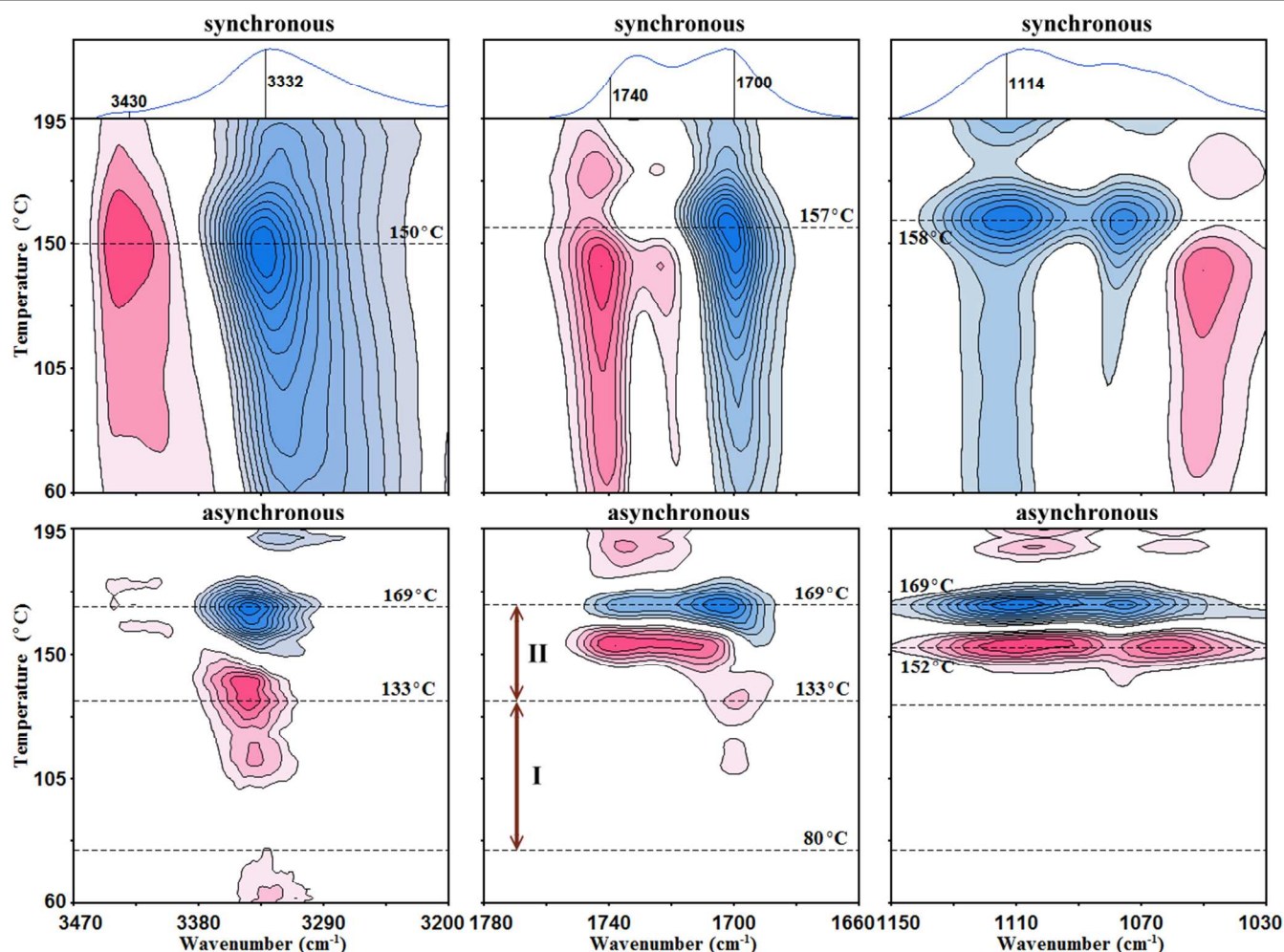
Figure 3. PCMW2D synchronous and asynchronous correlation FTIR spectra in the regions 3470–3200 cm^{-1}, 1780–1660 cm^{-1}, and 1150–1030 cm^{-1} calculated from the temperature-dependent FTIR spectra from 50 °C to 205 °C. In synchronous spectra, the horizontal dashed lines represent the temperature points at 150 °C, 157 °C, and 158 °C. In asynchronous spectra, the horizontal dashed lines correspond to the temperature points at 80 °C, 133 °C, 152 °C, and 169 °C, respectively. The pink areas represent positive correlation intensity, and the blue areas represent the negative.

3. Results and discussion

3.1. Temperature-dependent FTIR spectra upon heating

The temperature-dependent FTIR spectra of TPU upon heating from 50 °C to 205 °C in the region 3470−3200 cm^{-1}, 1810−1650 cm^{-1}, and 1160−990 cm^{-1} are shown in **Figure 1**. The assignments of peaks are listed in **Table 1**.[13-15, 23-28, 45, 46] The peaks of 3430 cm^{-1}, 3332 cm^{-1}, 1740 cm^{-1}, and 1700 cm^{-1} are attributed to TPU hard blocks.[13-15, 26, 45, 46] Specifically, the peak at 3430 cm^{-1} is assigned to N−H stretching of "free" N−H groups,[23, 26, 45] and peak at 3332 cm^{-1} is N−H stretching of hydrogen-bonded N−H groups.[13, 26] The peak at 1740 cm^{-1} is C=O stretching of "free" C=O groups,[13-15, 46] and 1700 cm^{-1} is assigned to C=O stretching of hydrogen-bonded C=O groups.[25, 26, 46] The peak at 1114 cm^{-1} is attributed to TPU soft blocks, which is derived from C−O−C asymmetrical stretching of polytetrahydrofuran.[14, 46] The change of these peaks illustrated in **Figure 1** arouses our interest, because it reveals the hydrogen bonds breaking. It can be observed that

the intensity of 3332 cm^{-1} obviously decreases, and that of 3430 cm^{-1} gradually enhances when the temperature increases from 50 °C to 205 °C. This indicates the breaking of hydrogen bonds relating to N−H groups (3332 cm^{-1}) and the generation of "free" N−H groups (3430 cm^{-1}). We can also observe that the intensity of 1700 cm^{-1} reduces to a disappearance, and that of 1740 cm^{-1} increases when heating from 50 °C to 205 °C. In addition, the peak of 1740 cm^{-1} significantly shifts to a higher wavenumber. This phenomenon also clearly shows the breaking of hydrogen bonds (1700 cm^{-1}) and the generation of "free" C=O groups (1740 cm^{-1}). At the same time, the intensity deceasing of 1114 cm^{-1} is also observed. As mentioned in the introduction of this paper, for TPUs, two types of hydrogen bonds can be generated. The main hydrogen bonds are formed between N–H and C=O groups in hard blocks due to the phase separation, and the minor hydrogen bonds are generated between N–H and C−O−C groups in the phase interface between the hard and soft blocks.[12-14, 46] Thus, the intensity decreasing of both 3332 cm^{-1} and 1700 cm^{-1} reveals the hydrogen bonds breaking between N–H and C=O

groups in hard blocks, and the intensity decreasing of 1114 cm^{-1} possibly represents the hydrogen bonds breaking between N–H and C–O–C groups in the phase interface.

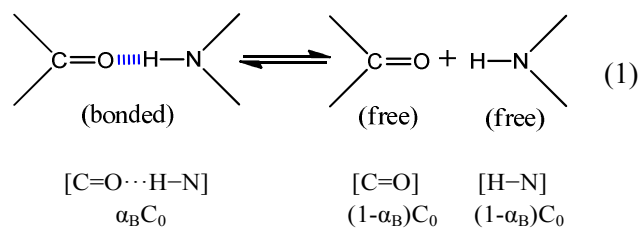### 3.2. Temperature regions of hydrogen bonds breaking determined from PCMW2D and DSC

DSC curve of TPU from 50 °C to 220 °C upon heating is illustrated in **Figure 2**. A broad endothermic peak within 60−180 °C is observed, which certainly derives from the melting of the crystalline in TPU hard blocks.[16, 47-49] It can be discerned that this broad peak is composed of several peaks. The temperature of the largest peak is determined at 151 °C, and other weak peaks cannot be accurately judged. According to the literature,[26, 28] hydrogen bonds are the main reason of the crystalline formation in TPU hard blocks, and therefore, such as the findings in temperature-dependent FTIR in **Figure 1,** the crystalline melting in DSC also directly reflects the hydrogen bonds breaking in TPU hard blocks. As shown in **Figure 2**, the onset point and the end point of the crystalline melting can be determined at 80 °C and 170 °C, respectively.

Figure 3 is the PCMW2D FTIR spectra calculated from the temperature-dependent FTIR of TPU from 50 °C to 205 °C. PCMW2D contains synchronous and asynchronous correlation spectra. The pink areas represent positive correlation intensity, and the blue areas represent the negative. For synchronous FTIR spectra, the negative correlation intensity indicates the decreasing of spectral intensity at a given wavenumber in the temperature-dependent spectra, and vice versa. Because of 3332 cm^{-1}, 1700 cm^{-1}, and 1114 cm^{-1} representing hydrogen bonding, we focus our discussions on these three bands. In **Figure 3**, for synchronous FTIR spectra, 3332 cm^{-1}, 1700 cm^{-1}, and 1114 cm^{-1} show the negative correlation intensity throughout the entire temperature range (60−195 °C), and this clearly indicates continuous hydrogen bonds breaking upon heating from 60 °C to 195 °C. In addition, the transition temperature of 3332 cm^{-1}, 1700 cm^{-1}, and 1114 cm^{-1} can be observed at 150 °C, 157 °C, and 158 °C, respectively. The asynchronous FTIR spectra can be easily used to determine the temperature region of polymer transitions.[38-44] As shown in **Figure 3**, the temperature regions of bands at 3332 cm^{-1} and 1700 cm^{-1} are both 133−169 °C. However, a narrower temperature region of 1114 cm^{-1} is observed within 152−169 °C. For these temperature regions, the maximum point 169 °C is very close to the end point at 170 °C determined by DSC curve. In **Figure 3**, from the temperature regions of bands at 3332 cm^{-1} and 1700 cm^{-1} (133−169 °C), using the lowest point 133 °C can determine a boundary for the crystalline melting induced by hydrogen bonds breaking in TPU hard blocks, which is also labelled in **Figure 2**. Thus, the PCMW2D FTIR spectra determine a temperature region of 133−169 °C. Combined with DSC, because the onset point is determined at 80 °C, another temperature region can be determined from 80 °C to 133 °C. As shown in **Figure 2** and **Figure 3**, two temperature regions of the crystalline melting induced by hydrogen bonds breaking, called region I (80−133 °C) and region II (133−169 °C), are

ascertained. Actually, the endothermic peak within 80−133 °C in DSC is the imperfect crystalline melting in TPU hard blocks, the endothermic peak within 133−169 °C is the perfect crystalline melting, which will be discussed in the following section.

3.3. Enthalpy of hydrogen bonds breaking estimated from FTIR

The breaking and generation of hydrogen bonds between C=O and N−H groups can be considered as an equilibrium reaction:

$$\quad (1)$$

(bonded)   (free)   (free)

$$[C=O\cdots H−N] \qquad\qquad [C=O] \qquad [H−N]$$
$$\alpha_B C_0 \qquad\qquad\qquad (1-\alpha_B)C_0 \quad (1-\alpha_B)C_0$$

where $[C=O\cdots H−N]$ is the molar concentration of hydrogen bonded groups between C=O and N−H, and $[C=O]$, $[H−N]$ are the molar concentration of free C=O and free H−N groups, respectively.

According to Beer-Lambert Law, the following relationship exists:

$$A = \varepsilon L C \qquad (2)$$

where A is absorbance, and C is the molar concentration. The ε is the extinction coefficient, and L is the optical path of the sample.

Here, we suppose the total molar concentration of hydrogen bonded C=O groups is C_0 at a lower temperature T_l. The C_B and C_F are the molar concentration of hydrogen bonded C=O groups and free C=O groups, respectively. As the temperature increasing, the hydrogen bonds breaking will make the bonded C=O groups gradually transform into free C=O groups, and the relationship of C_0, C_B, and C_F is:

$$C_B + C_F = C_0 \qquad (3)$$

According to Beer-Lambert Law:

$$A_0 = \varepsilon_B L C_0 \qquad (4)$$

$$A_B = \varepsilon_B L C_B \qquad (5)$$

$$A_F = \varepsilon_F L C_F \qquad (6)$$

where ε_B is the extinction coefficient of the bonded C=O groups, and ε_F is the extinction coefficient of free C=O groups. At a given temperature, the molar fraction of the bonded C=O groups is:

$$\alpha_B = \frac{C_B}{C_0} = \frac{A_B / \varepsilon_B L}{A_0 / \varepsilon_B L} = \frac{A_B}{A_0} \qquad (7)$$

Similarly, the mole fraction of free C=O groups can be expressed by the equation (8):

$$\alpha_F = \frac{C_F}{C_0} = \frac{C_0 - C_B}{C_0} = 1 - \alpha_B \quad (8)$$

So, the equation (9) can be used to calculate the equilibrium constant of the equation (1).

$$K = \frac{[C=O][H-N]}{[C=O\cdots H-N]} = \frac{(1-\alpha_B)^2 C_0}{\alpha_B} \quad (9)$$

We transform the equation (9) into Van't Hoff form:

$$\ln K = \ln[\frac{(1-\alpha_B)^2}{\alpha_B}] + \ln C_0 = -\frac{\Delta H_h}{R} \cdot \frac{1}{T} + \frac{\Delta S}{R} \quad (10)$$

$$\ln[\frac{(1-\alpha_B)^2}{\alpha_B}] = -\frac{\Delta H_h}{R} \cdot \frac{1}{T} + \frac{\Delta S}{R} - \ln C_0 \quad (11)$$

where R is the gas constant (8.314 J/mol·K), and T is the absolute temperature (in Kelvin). ΔH_h is the enthalpy of hydrogen bonds breaking (J/mol), and ΔS is entropy (J/mol·K).

So, the least squares fitting can be used to fit a straight line of the plot between $\ln[(1-\alpha_B)^2/\alpha_B]$ and $1/T$. The enthalpy of hydrogen bonds breaking of C=O···H−N can be easily gained from the slope of the fitted straight line.
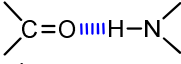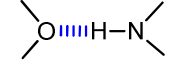
The enthalpy of hydrogen bonds breaking between C−O−C and H−N can also be estimated from the same manner as described above from the following equilibrium reaction:

$$(12)$$

(bonded)   (free)   (free)
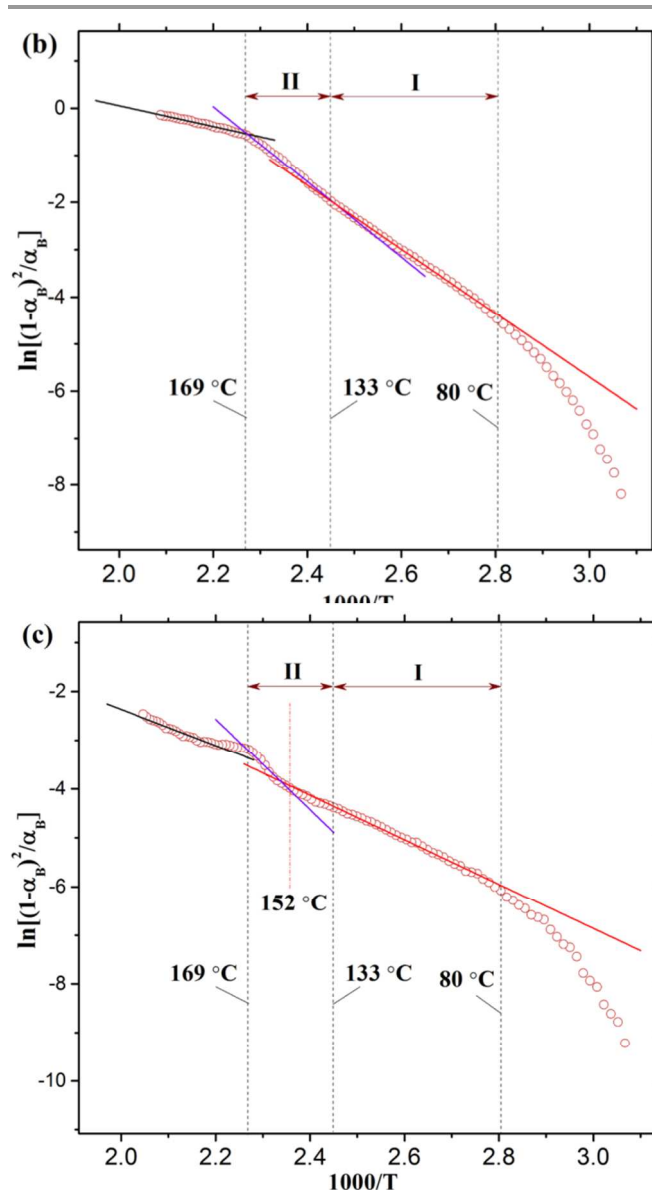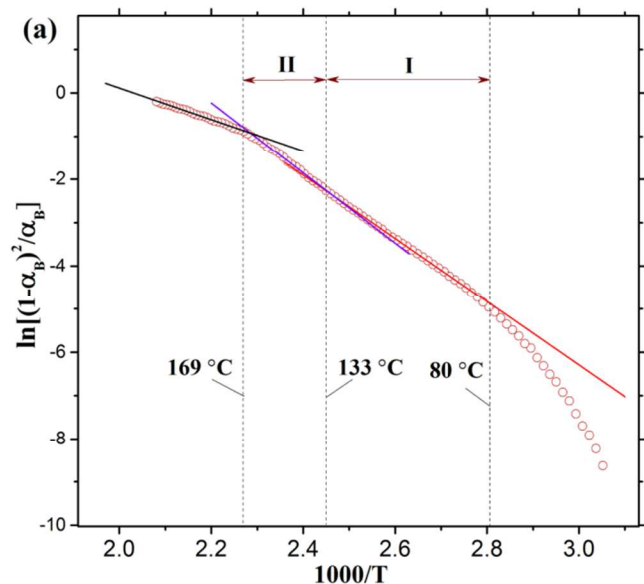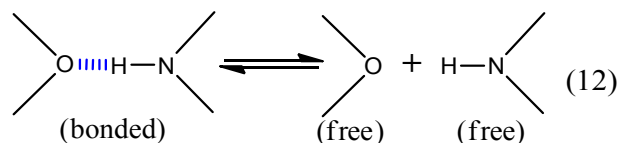
Figure 4. Van't Hoff plots from the temperature-dependent FTIR of TPU. (a) Calculating from the absorbance change at 3332 cm^{-1}, which represents the breaking of hydrogen bonds of all types generated from N−H groups; (b) Calculating from the absorbance change at 1700 cm^{-1}, which represents hydrogen bonds breaking between N−H and C=O groups; (c) Calculating from the absorbance change at 1114 cm^{-1}, which represents hydrogen bonds breaking between N−H and C−O−C groups.

Figure 4(a), **Figure 4(b)**, and **Figure 4(c)** show Van't Hoff plots calculated from the temperature-dependent FTIR at 3332 cm^{-1}, 1700 cm^{-1}, and 1114 cm^{-1}, respectively. The bands at 3332 cm^{-1} is assigned to hydrogen-bonded N−H groups. Because N−H groups are only hydrogen bonding donor in TPU, all types of hydrogen bonds are generated from N−H groups. Thus, Van't Hoff analysis of 3332 cm^{-1} can conveniently estimate the average enthalpy of the breaking of all hydrogen bonds types. For TPU, both C−O−C and C=O groups are hydrogen bonding acceptors, and the bands at 1700 cm^{-1} and 1114 cm^{-1} are attributed to hydrogen-bonded C=O

Table 2. The enthalpies of hydrogen bonds breaking calculated from Van't Hoff plots in **Figure 4**.

Hydrogen bond types	Enthalpy of hydrogen bonds breaking, ΔH_h (kJ/mol)			Composition of hydrogen bonds (mol%)		
	Region I (80-133 °C)	Region II (133-169 °C)	169-205 °C	Region I (80-133 °C)	Region II (133-169 °C)	169-205 °C
All types (average)	56.3±0.2	67.3±0.9	29.9±0.4	100.0	100.0	100.0
C=O⋯H−N	58.8±0.5	65.0±1.1	19.3±0.4	88.4	71.2	22.6
O⋯H−N	37.2±0.4	73.0±3.9	33.0±1.3	11.6	28.8	77.4

and C−O−C groups, respectively. So, from the Van't Hoff analysis of 1700 cm^{-1} and 1114 cm^{-1}, the enthalpies of hydrogen bonds breaking of these two hydrogen bonds (N−H and C=O, N−H and C−O−C) can also be calculated. As shown in **Figure 4**, two temperature regions, which have been confirmed through DSC and PCMW2D, can also be determined from Van't Hoff plots.

In **Figure 4**, three straight lines are successfully fitted for each Van't Hoff plot, which indicates that three enthalpies can be calculated upon heating. We list these estimated enthalpies in **Table 2**. For hydrogen bonds breaking, an endothermic process is observed due to the positive value of the calculated enthalpies. Thus, a larger absolute value of the enthalpy represents a more difficulty of hydrogen bonds breaking. In region I (80-133 °C), the enthalpy of hydrogen bonds breaking (ΔH_h) between N−H and C=O groups is 58.8±0.5 kJ/mol, and that of N−H and C−O−C groups is 37.2±0.4 kJ/mol. This indicates that hydrogen bonds breaking of N−H and C−O−C are much more easy than that of N−H and C=O when the temperature is within 80-133 °C. In region II (133-169 °C), ΔH_h=65.0±1.1 kJ/mol for hydrogen bonds of N−H and C=O, and ΔH_h=73.0±3.9 kJ/mol for hydrogen bonds of N−H and C−O−C groups. Instead, hydrogen bonds breaking of N−H and C−O−C groups is slightly more difficult than that of N−H and C=O within 133-169 °C, which is different from region I. A similar phenomenon is also observed when the temperature is within 169-205 °C (above region II), because ΔH_h=19.3±0.4 kJ/mol for hydrogen bonds between N−H and C=O, and ΔH_h=33.0±1.3 kJ/mol for that of N−H and C−O−C.

For hydrogen bonds of N−H and C=O, ΔH_h first enhances from 58.8±0.5 kJ/mol to 65.0±1.1 kJ/mol as the temperature increasing from region I (80-133 °C) to region II (133-169 °C), and then it suddenly drops to 19.3±0.4 kJ/mol when temperature is further increased to 169-205 °C. In general, the imperfect crystalline in TPU hard blocks is induced by irregular hydrogen bonds of N−H and C=O,[13-15] and the regular hydrogen bonds of N−H and C=O always lead to the perfect crystalline.[13-15] In this study, the irregular hydrogen bonds of N−H and C=O induce TPU hard blocks to form series of the imperfect crystalline which present a continuous melting within 80-133 °C in DSC (**Figure 2**). Thus, the breaking enthalpy (58.8±0.5 kJ/mol) in Region I reveals the breaking of irregular hydrogen bonds of N−H and C=O, and therefore presenting a lower ΔH_h. In contrast, in Region II, because of a higher ΔH_h (65.0±1.1 kJ/mol), the bonds

breaking is ascribed to regular hydrogen bonds of N−H and C=O, and the induced perfect crystalline in TPU hard blocks presents a highest melting peak at 151 °C in DSC curve. After Region II, ΔH_h=19.3±0.4 kJ/mol shows the existence of little hydrogen bonds of N−H and C=O.

For hydrogen bonds between N−H and C−O−C, a similar feature of the first increases and then decreases is observed. In region I, because of ΔH_h=37.2±0.4 kJ/mol showing an easy trend of the bonds breaking, it can be inferred that only a small amount of hydrogen bonds of N−H and C−O−C exist. The estimated ΔH_h is also in line with our common sense that hydrogen bonds between N−H and C−O−C are unstable. In region II, ΔH_h gives a surprised high value of 73.0±3.9 kJ/mol, even 8 kJ/mol higher than the enthalpy of N−H and C=O (65.0±1.1 kJ/mol), which is inconsistent with our common sense that hydrogen bonds of N−H and C=O are much more stable than that of N−H and C−O−C. The enthalpy clearly shows that the stability of hydrogen bonds of N−H and C=O is even worse than that of N−H and C−O−C. At first, we thought it must be a calculation error. However, after several attempts, we finally confirmed that this value was correct. In addition, in **Table 2**, it can be observed the average enthalpy for all hydrogen bonds types is calculated as 67.3±0.9 kJ/mol which is between 65.0±1.1 kJ/mol and 73.0±3.9 kJ/mol. If the value 73.0±3.9 kJ/mol is an error (for example, less than 65.0 kJ/mol), the average enthalpy should be less than 65.0 kJ/mol. However, what causes such a high enthalpy of hydrogen bonds breaking between N−H and C−O−C in region II? This brings us a confusion. As far as we knew, TPU is a block copolymer with a micro-phase separation structure. According to the literature,[16, 19] there exists an order-disorder transition (ODT) for TPU at a high temperature within 120-170 °C. In general, the occurrence of this ODT transition is immediately after the crystalline melting of TPU hard blocks, which is actually the molecular chain disentangling in hard blocks and a full mixing with the molecular chains of soft blocks, resulting in the disappearance of the phase separation structure and the formation of a uniform melt. The ODT transition which is an endothermic process needs to overcome the repulsion energy (also known as the interaction energy) between hard and soft blocks. Like other block polymers, the repulsion energy mainly appears in the phase interface, where is the only place of existing hydrogen bonds of N−H and C−O−C. This explains why a high enthalpy exhibits for hydrogen bonds breaking of N−H and C−O−C in region II.
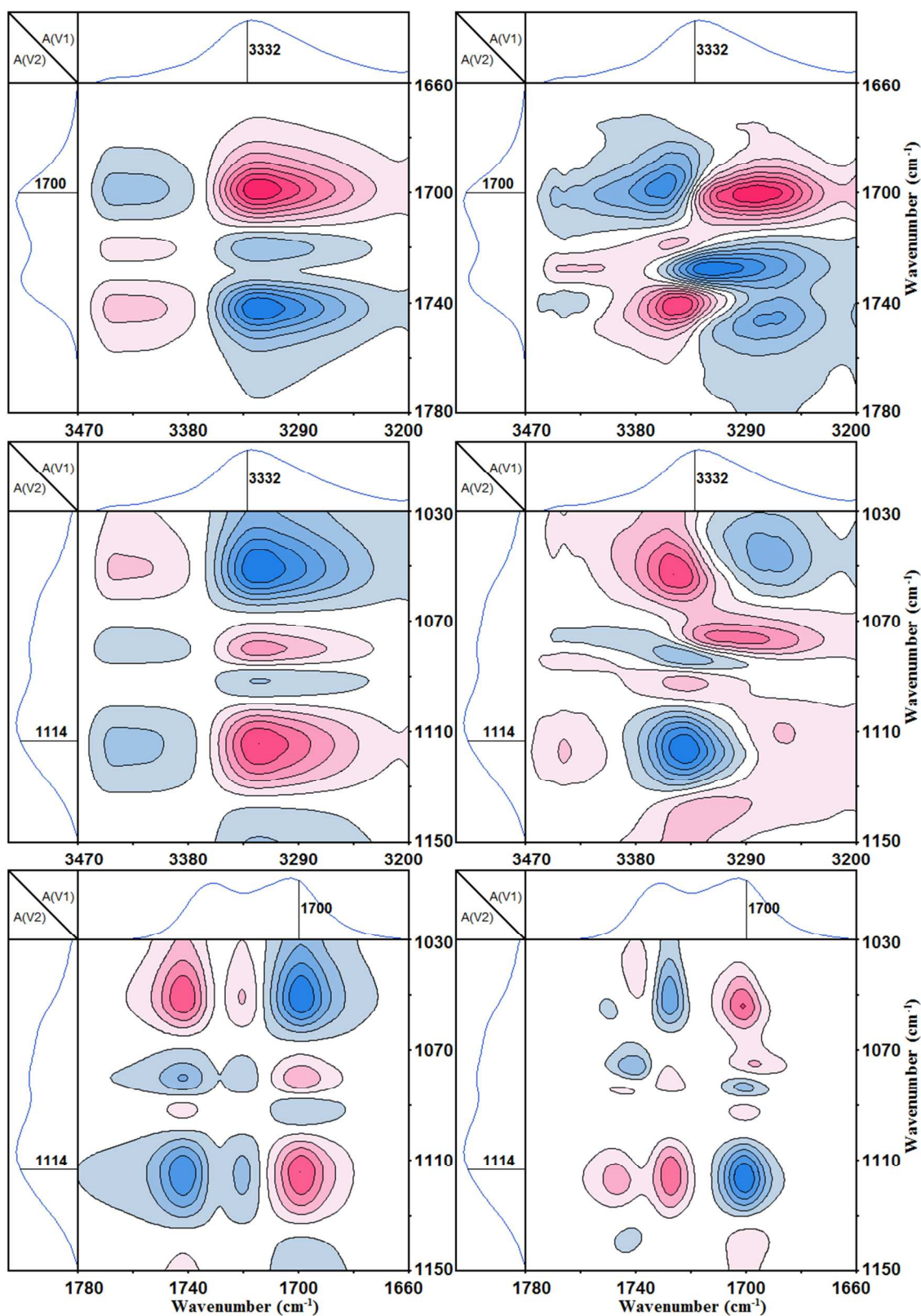
Figure 5. Synchronous (left) and asynchronous (right) FTIR spectra calculated from temperature-dependent spectra of region I (80–133 °C) in the region 3470–3200 cm^{-1} *vs* 1780–1660 cm^{-1}，3470–3200 cm^{-1} *vs* 1150–1030 cm^{-1}, and 1780–1660 cm^{-1} *vs* 1150–1030 cm^{-1}. Pink and blue areas represent the positive and negative correlation intensity, respectively.

The enthalpy of hydrogen bonds breaking of N–H and C−O−C actually reflects the stabilizing effect of the repulsion energy on hydrogen bonds in the interface. After region II, for hydrogen bonds of N–H and C−O−C, ΔH_h=33.0±1.3 kJ/mol is obtained, and it is still higher than that of N–H and C=O (33.0±1.3 kJ/mol).

Here, a method is proposed for TPU to calculate the composition of hydrogen bonds in different temperature regions using the average enthalpy for all hydrogen bonds types.

Supposing X is the relative amount of hydrogen bonds of N–H and C=O, and Y is the relative amount of hydrogen bonds of N–H and C−O−C. So, we give the following two element equations:

$$\Delta H_{h-X} X + \Delta H_{h-Y} Y = \Delta H_{h-average} \qquad (13)$$

$$X+Y=1 \qquad (14)$$

where ΔH_{h-X} is the enthalpy of hydrogen bonds breaking of N–H and C=O, and ΔH_{h-Y} is the enthalpy of hydrogen bonds breaking of N–H and C−O−C. $\Delta H_{h-average}$ is the average enthalpy of hydrogen bonds breaking for all types. The X and Y can be easily calculated through above equations, and results are also listed in **Table 2**.

In region I, the percentage of hydrogen bonds of N–H and C=O is 88.4%, and that of N–H and C−O−C is 11.6%. In region II, above two values are 71.2 % and 28.8%, respectively. This reveals that the hydrogen bonds are mainly between N–H and C=O groups, and hydrogen bonds between N–H and C−O−C has only a small part when the temperature is below 169 °C. Instead, after region II, the amount of hydrogen bonds of N–H and C=O (22.6%) is much lower than that of N–H and C−O−C (77.4%). However, within 169-205 °C, although the relative amount of hydrogen bonds can be calculated, it cannot be denied that the total number of hydrogen bonds in the TPU melt is very small at such a high temperature due to the low enthalpy.

From the discussions above, the physical meanings of region I and II can be clearly determined. Briefly, region I is almost the irregular hydrogen bonds breaking of N–H and C=O in TPU hard blocks and is accompanied by a small amount of hydrogen bonds breaking of N–H and C−O−C in the interface. Region II is firstly the regular hydrogen bonds breaking of N–H and C=O in TPU hard blocks, and then is followed by the ODT transition which needs to overcome hydrogen bonds of N–H and C−O−C and the repulsion energy in the interface.

3.4. Generalized 2D correlation analysis

In order to understand hydrogen bonds breaking for TPU from the molecular movements, the temperature-dependent FTIR spectra within region I (80-133 °C) and II (133-169 °C) were used to perform the generalized 2D correlation analysis. Using Noda's rules, the sequential order of the spectral intensity change can be conveniently determined by the sign

of the correlation peaks. Noda's rules are summarized as follows:[29, 30]

1) If $\Phi(v_1, v_2)>0$, $\Psi(v_1, v_2)>0$ or $\Phi(v_1, v_2)<0$, $\Psi(v_1, v_2)<0$, then the movement of v_1 is before that of v_2;

2) If $\Phi(v_1, v_2)>0$, $\Psi(v_1, v_2)<0$ or $\Phi(v_1, v_2)<0$, $\Psi(v_1, v_2)>0$, then the movement of v_1 is after that of v_2;

3) If $\Phi(v_1, v_2)>0$, $\Psi(v_1, v_2)=0$ or $\Phi(v_1, v_2)<0$, $\Psi(v_1, v_2)=0$, then the movements of v_1 and v_2 are simultaneous.
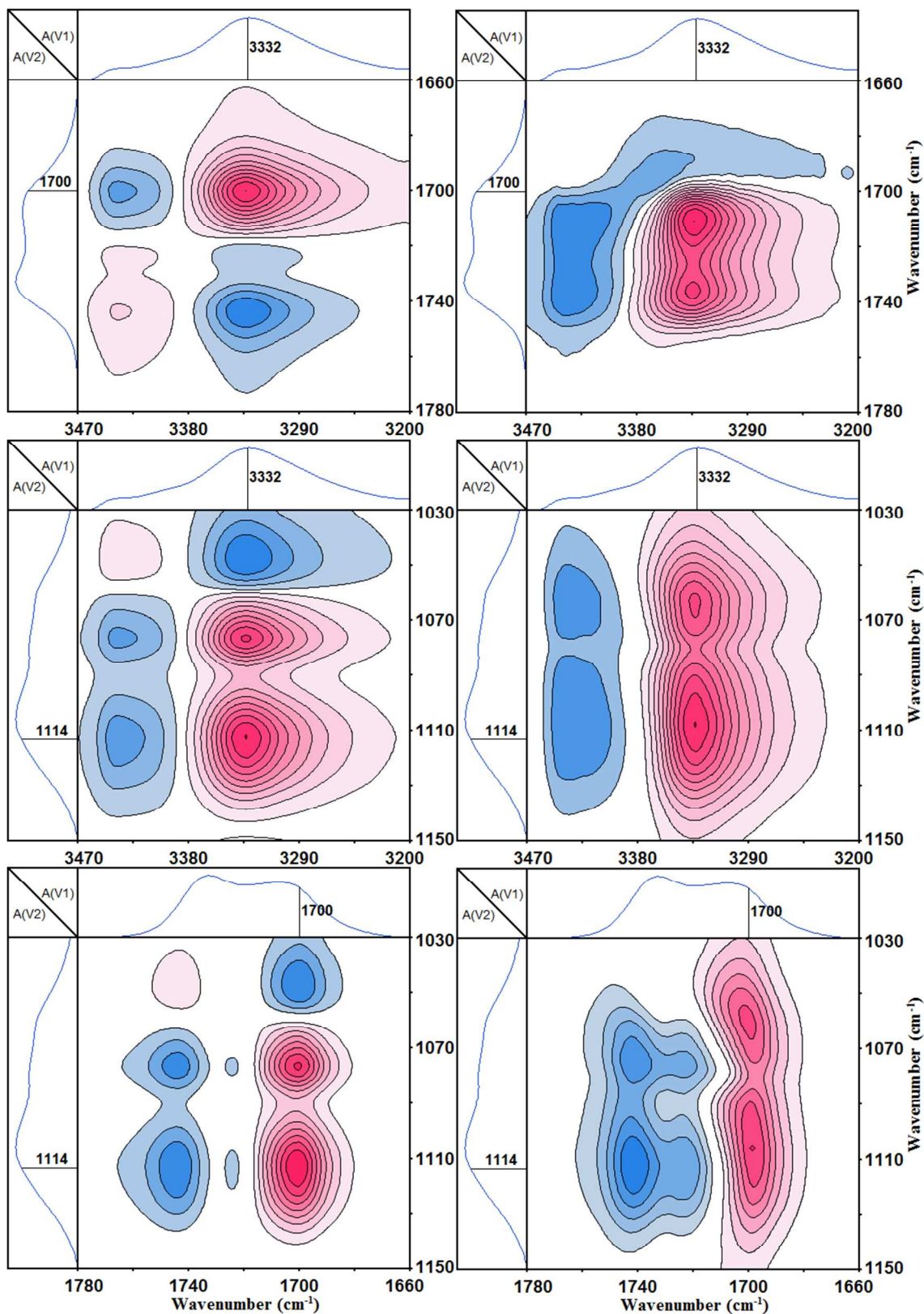
Table 3. Sequential order of the bands of bonded N−H groups, bonded C=O groups, and C−O−C groups, obtained from **Figure 5**.

Cross correlation peak (cm^{-1}, cm^{-1})	Sign in synchronous spectra	Sign in asynchronous spectra	Sequential order
(3332, 1700)	+	+	3332→1700
(3332, 1114)	+	-	3332←1114
(1700, 1114)	+	-	1700←1114
1114→3332→1700			
v_{as}(C−O− C, soft block)→v(N−H, bonded)→v(C=O, bonded)			

3.4.1. Sequential order of the breaking of hydrogen bonded groups in region I

Figure 5 is the generalized 2D correlation FTIR spectra in the region 3470−3200 cm^{-1} vs 1780−1660 cm^{-1}, 3470−3200 cm^{-1} vs 1150−1030 cm^{-1}, and 1780−1660 cm^{-1} vs 1150−1030 cm^{-1}, which is calculated from temperature-dependent spectra of region I (80−133 °C). The generalized 2D correlation FTIR contains both synchronous and asynchronous spectra. In **Figure 5**, the left are the synchronous spectra, and the right are the asynchronous spectra. The pink areas represent the positive correlation intensity, and the blue areas are the negative correlation intensity. The signs of the correlation peaks of 3332 cm^{-1}, 1700 cm^{-1}, and 1114 cm^{-1} are summarized in **Table 3**. The sequential order is gained as 1114 cm^{-1}→3332 cm^{-1}→1700 cm^{-1} according to Noda's rules. In the present study, the symbol "→" represents "before", and "←" represents "after". The corresponding sequential order of the movements of hydrogen bonded groups is v_{as}(C−O−C, soft block)→v(N−H, bonded)→v(C=O, bonded). Clearly, for region I, the first step of the molecular movement is C−O−C groups, representing TPU soft blocks. Then, the molecular movement of hard blocks occurs. Thus, the second step is the movement of hydrogen bonded N−H groups in hard blocks, and the third step is that of hydrogen bonded C=O groups (also in hard blocks). As the discussed in the previous sections, the hydrogen bonds of N−H and C−O−C groups are located in the interface, and the irregular hydrogen bonds of N−H and C=O groups induce to form the imperfect crystalline in hard blocks. Thus, from the molecular movements, it can be easily inferred that the first step is the breaking of the hydrogen bonds of N−H and C−O−C groups in the interface. Because the last two steps are the molecular movements in TPU hard blocks, these two steps are all attributed to the breaking of hydrogen bonds of N−H and C=O groups in the imperfect crystalline of hard blocks. From the 2D correlation analysis, the breaking of hydrogen bonds of N−H and C−O−C groups is

obviously ahead that of N−H and C=O groups. This result is also consistent with the findings from the enthalpy in **Table 2**.

Figure 6. Synchronous (left) and asynchronous (right) FTIR spectra calculated from temperature-dependent spectra of region II (133–169 °C) in the region 3470–3200 cm^{-1} *vs* 1780–1660 cm^{-1}, 3470–3200 cm^{-1} *vs* 1150–1030 cm^{-1}, and 1780–1660 cm^{-1} *vs* 1150–1030 cm^{-1}.

Table 4. Sequential order of the bands of bonded N−H groups, bonded C=O groups, and C−O−C groups, obtained from **Figure 6**.

Cross correlation peak (cm⁻¹, cm⁻¹)	Sign in synchronous spectra	Sign in asynchronous spectra	Sequential order
(3332, 1700)	+	+	3332→1700
(3332, 1114)	+	+	3332→1114
(1700, 1114)	+	+	1700→1114
3332→1700→1114			
v(N−H, bonded)→v(C=O, bonded)→v_{as}(C−O−C, soft block)			

3.4.2. Sequential order of the breaking of hydrogen bonded groups in region II

The generalized 2D correlation FTIR spectra in the region 3470−3200 cm⁻¹ vs 1780−1660 cm⁻¹, 3470−3200 cm⁻¹ vs 1150−1030 cm⁻¹, and 1780−1660 cm⁻¹ vs 1150−1030 cm⁻¹ are shown in **Figure 6**, which are calculated from temperature-dependent spectra of region II (133−169 °C). The signs of the correlation peaks of 3332 cm⁻¹, 1700 cm⁻¹, and 1114 cm⁻¹ are summarized in **Table 4**. According to Noda's rules, the sequential order is 3332 cm⁻¹→1700 cm⁻¹→1114 cm⁻¹. Thus, the sequential order of the groups movement is v(N−H, bonded)→v(C=O, bonded)→v_{as}(C−O−C, soft block). The previous two steps are the breaking of hydrogen bonds of N−H and C=O groups in perfect crystalline of hard blocks, and the last step is the breaking of the hydrogen bonds of N−H and C−O−C groups in the interface, resulting in the order-disorder transition. In **Table 2**, ΔH_h=73.0±3.9 kJ/mol for the hydrogen bonds of N−H and C−O−C groups, and ΔH_h=65.0±1.1 kJ/mol for the hydrogen bonds of N−H and C=O groups. In region II, the enthalpy indicates the hydrogen bonds breaking of N−H and C−O−C groups is more difficult than that of N−H and C=O groups, which is the same as the inferred from the 2D correlation analysis.
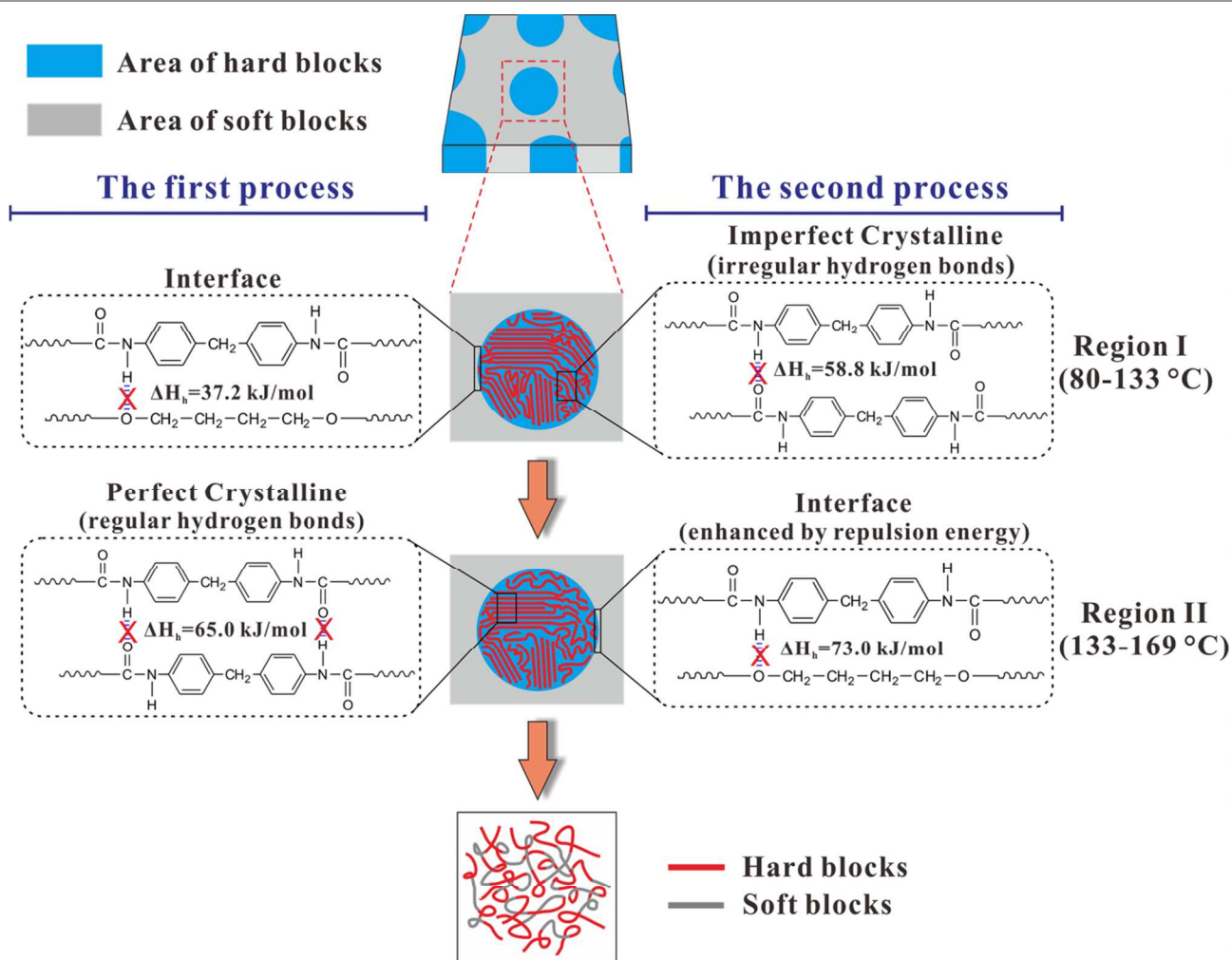
Scheme 2. The detailed information of region I and region II inferred from the 2D correlation analysis. The blue areas represent the domain formed by TPU hard blocks, and the gray areas represent the domain formed by TPU soft blocks.

Scheme 2 illustrates the detailed information of region I and region II inferred from the 2D correlation analysis. The blue areas represent the domain formed by TPU hard blocks, and the gray areas represent the domain formed by TPU soft blocks. For Region I (80−133 °C), the breaking of the irregular hydrogen bonds between N–H and C=O in TPU hard

blocks is dominated, resulting in the melting of the imperfect crystalline in TPU hard blocks. In addition, the breaking of a small amount of hydrogen bonds between N–H and C−O−C in the interface also occurs. In Region I, the first process is the breaking of unstable hydrogen bonds of N–H and C−O−C, and the second process is the breaking of hydrogen bonds of N–H and C=O. For Region II (133−169 °C), the first process is the breaking of regular hydrogen bonds between N–H and C=O in the perfect crystalline in TPU hard blocks, and the second process is the breaking of hydrogen bonds of N–H and C−O−C enhanced by the repulsion energy in the interface. The second process eventually leads to the ODT transition of TPU.

4. Conclusions

In this study, the hydrogen bonds breaking of TPU based on MDI/BDO upon heating was studied and elucidated from the viewpoint of molecular movements and enthalpy.

Two temperature regions of hydrogen bonds breaking for TPU, including region I (80−133 °C) and region II (133−169 °C), were determined via the combination of PCMW2D and DSC. The method of calculating the enthalpy of the hydrogen bonds breaking was established via Van't Hoff plots from the absorbance change of temperature-dependent FTIR. The relationship of the breaking enthalpies of different hydrogen bonds type was also proposed, and therefore, the relative content of hydrogen bonds of N–H and C=O groups, as well as that of N–H and C−O−C, can be calculated quantitatively. In region I, ΔH_h of N–H and C=O groups is 58.8±0.5 kJ/mol, and that of N–H and C−O−C groups is 37.2±0.4 kJ/mol. The relative content of hydrogen bonds of N–H and C=O is 88.4%, and that of N–H and C−O−C is 11.6%. In region II, ΔH_h=65.0±1.1 kJ/mol for hydrogen bonds of N–H and C=O, and ΔH_h=73.0±3.9 kJ/mol for hydrogen bonds of N–H and C−O−C groups. The relative contents of these two hydrogen bonds are 71.2 % and 28.8%, respectively. The surprised high value of ΔH_h=73.0±3.9 kJ/mol for hydrogen bonds of N–H and C−O−C groups in region II is probably due to the stabilization of the repulsion energy on hydrogen bonds in the interface. From Van't Hoff plots, the temperature regions of region I and region II were further confirmed within 80−133 °C and 133−169 °C, respectively.

The 2D correlation analysis was used to investigate the sequential order of groups' movement involved in hydrogen bonds breaking. In Region I, the breaking of a small amount of hydrogen bonds between N–H and C−O−C in the interface firstly occurs, and then the breaking of the irregular hydrogen bonds between N–H and C=O in TPU hard blocks is dominated, resulting in the melting of the imperfect crystalline in TPU hard blocks. In Region II, it is firstly the regular hydrogen bonds breaking between N–H and C=O in the perfect crystalline in TPU hard blocks, and then is followed by the breaking of hydrogen bonds of N–H and C−O−C enhanced

by the repulsion energy in the interface, leading to the ODT transition of TPU.
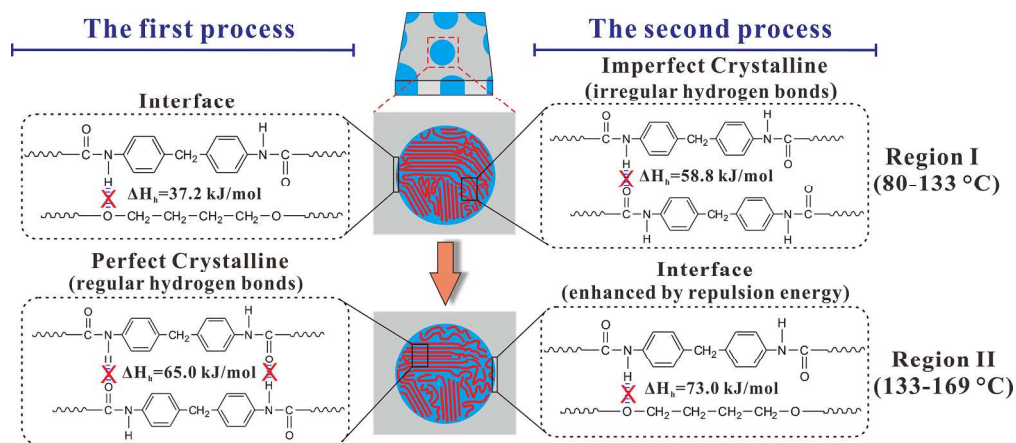
Acknowledgements

Notes and references

[a] State Key Laboratory of Polymer Materials Engineering of China, Polymer Research Institute, Sichuan University, Chengdu 610065, China

[b] State Key Laboratory of High Performance Civil Engineering, Jiangsu Subute New Materials Co., Ltd, Nanjing 211103, China

*Corresponding author. Tel.: +86-28-85402601; Fax: +86-28-85402465; E-mail address: zhoutaopoly@scu.edu.cn (T. Zhou)

1. A. K. Bhowmick, H. L.S tephens, *Handbook of Elastomers*. 2nd ed.; Marcel Dekker, Inc.: New York, 2000.
2. S. Fakirov, *Handbook of Condensation Thermoplastic Elastomers*. WILEY-VCH Verlag GmbH & Co. KGaA: Weinheim, 2005.
3. C. Furtado, G. G. Silva, J. Machado, M. Pimenta, R. Silva, *J. Phys. Chem. B*, 1999, **103**, 7102-7110.
4. X. Wang, Y. Hu, L. Song, H. Yang, W. Xing, H. Lu, *J. Mater. Chem.* 2011, **21**, 4222-4227.
5. A. F. Osman, G. A. Edwards, T. L. Schiller, Y. Andriani, K. S. Jack, I. C. Morrow, P. J. Halley, D. J. Martin, *Macromolecules*, 2011, **45**, 198-210.
6. J. Yang, Y. Gao, J. Li, M. Ding, F. Chen, H. Tan, Q. Fu, *RSC Adv.*, 2013, **3**, 8291-8297.
7. B. R. Nair, V. G. Gregoriou, P. T. Hammond, *J. Phys. Chem. B*, 2000, **104**, 7874-7880.
8. W. Li, A. J. Ryan, I. K. Meier, *Macromolecules*, 2002, **35**, 6306-6312.
9. V. G. Gregoriou, S. E. Rodman, B. R. Nair, P. T. Hammond, *J. Phys. Chem. B*, 2002, **106**, 11108-11113.
10. D. Ponnamma, K. K. Sadasivuni, M. Strankowski, P. Moldenaers, S. Thomas, Y. Grohens, *RSC Adv.*, 2013, **3**, 16068-16079.
11. D. J. Martin, G. F. Meijs, P. A. Gunatillake, S. J. Mccarthy, G. M. Renwick, *J. Appl. Polym. Sci.*, 1997, **64**, 803-817.
12. R. W. Seymour, S. L. Cooper, *Macromolecules*, 1973, **6**, 48-53.
13. C. S. P. Sung, N. Schneider, *Macromolecules*, 1975, **8**, 68-73.
14. L. Ning, W. De-Ning, Y. Sheng-Kang, *Macromolecules*, 1997, **30**, 4405-4409.
15. C. B. Aakeröy, K. R. Seddon, *Chem. Soc. Rev.*, 1993, **22**, 397-407.
16. A. Saiani, A. Novak, L. Rodier, G. Eeckhaut, J.-W. Leenslag, J. Higgins, *Macromolecules*, 2007, **40**, 7252-7262.
17. J. T. Koberstein, T. P. Russell, *Macromolecules*, 1986, **19**, 714-720.
18. T. Zhou, Z. Wu, Y. Li, J. Luo, Z. Chen, J. Xia, H. Liang, A. Zhang, *Polymer*, 2010, **51**, 4249-4258.

RSC Advances Accepted Manuscript

19. A. J. Ryan, C. W. Macosko, W. Bras, *Macromolecules*, 1992, **25**, 6277-6283.

20. R. L. McKiernan, A. M. Heintz, S. L. Hsu, E. D. Atkins, J. Penelle, S. P. Gido, *Macromolecules*, 2002, **35**, 6970-6974.

21. E. Yılgör, I. Yılgör, E. Yurtsever, *Polymer*, 2002, **43**, 6551-6559.

22. B. S. Lee, B. C. Chun, Y.-C. Chung, K. I. Sul, J. W. Cho, *Macromolecules*, 2001, **34**, 6431-6437.

23. M. M. Coleman, K. H. Lee, D. J. Skrovanek, P. C. Painter, *Macromolecules*, 1986, **19**, 2149-2157.

24. B. Nair, V. Gregoriou, P. Hammond, *Polymer*, 2000, **41**, 2961-2970.

25. S. Pongkitwitoon, R. Hernández, J. Weksler, A. Padsalgikar, T. Choi, J. Runt, *Polymer*, 2009, **50**, 6305-6311.

26. C.Bru te, S. Hsu, W. MacKnight, *Macromolecules*, 1982, **15**, 71-77.

27. M. M. Coleman, D. J. Skrovanek, J. Hu, P. C. Painter, *Macromolecules*, 1988, **21**, 59-65.

28. I. Yilgor, E. Yilgor, I. G. Guler, T. C. Ward, G. L. Wilkes, *Polymer*, 2006, **47**, 4105-4114.

29. I. Noda, *Appl. Spectrosc.*, 1993, **47**, 1329-1336.

30. I. Noda, Y. Ozaki, *Two-Dimensional Correlation Spectroscopy – Applications in Vibrational and Optical Spectroscopy*. John Wiley & Sons, Ltd: 2005.

31. M. Thomas, H. H. Richardson, *Vib. Spectrosc.*, 2000, **24**, 137-146.

32. S. Morita, H. Shinzawa, I. Noda, Y. Ozaki, *Appl. Spectrosc.,* 2006, **60**, 398-406.

33. W. Li, B. Sun, P. Wu, *Carbohyd. Polym.*, 2009, **78**, 454-461.

34. B. Zhang, H. Tang, P. Wu, *Polym. Chem.*, 2014, **5**, 5967-5977.

35. S. Sun, P. Wu, *Macromolecules,* 2012, **46**, 236-246.

36. L. Peng, T. Zhou, Y. Huang, L. Jiang, Y. Dan, *J. Phys. Chem. B,* 2014, **118**, 9496-9506.

37. B. Tang, P. Wu, H. Siesler, *J. Phys. Chem. B,* 2008, **112**, 2880-2887.

38. B. Zhang, H. Tang, P. Wu, *Macromolecules*, 2014, **47**, 4728-4737.

39. L. Hou, K. Ma, Z. An, P. Wu, *Macromolecules*, 2014, **47**, 1144-1154.

40. X. Liu, T. Zhou, Y. Liu, A. Zhang, C. Yuan, W. Zhang, *RSC Adv.*, 2015, **5**, 10231-10242.

41. T. Zhou, L. Peng, Y. Liu, Y. Zhan, F. Liu, A. Zhang, *Vib. Spectrosc.*, 2014, **70**, 137-161.

42. B. Sun, Y. Lin, P. Wu, H. W. Siesler, *Macromolecules*, 2008, **41**, 1512-1520.

43. Y. Li, T. Zhou, Z. Chen, J. Hui, L. Li, A. Zhang, *Polymer*, 2011, **52**, 2059-2069.

44. Y. Chen, X. Sun, C. Yan, Y. Cao, T. Mu, *J. Phys. Chem. B*, 2014, **118**, 11523-11536.

45. G. Senich, W. MacKnight, *Macromolecules*, 1980, **13**, 106-110.

46. A. Ferry, P. Jacobsson, J. Van Heumen, J. Stevens, *Polymer*, 1996, **37**, 737-744.

47. S. Yamasaki, D. Nishiguchi, K. Kojio, M. Furukawa, *Polymer*, 2007, **48**, 4793-4803.

48. Y. Yanagihara, N. Osaka, S. Murayama, H. Saito, *Polymer*, 2013, **54**, 2183-2189.

49. C. Li, J. Liu, J. Li, F. Shen, Q. Huang, H. Xu, *Polymer*, 2012, **53**, 5423-5435.

184x79mm (300 x 300 DPI)